Peter Wolf, Sébastien Bize, André Clairon, Giorgio Santarelli, Michael E. Tobar and André N. Luiten
Improved test of Lorentz invariance in electrodynamics

Improved test of Lorentz invariance in electrodynamics

Peter Wolf,* Sébastien Bize, André Clairon, and Giorgio Santarelli

BNM-SYRTE, Observatoire de Paris, 61 Avenue de l'Observatoire, 75014 Paris, France

Michael E. Tobar and André N. Luiten

School of PhysicsUniversity of Western Australia, Crawley 6009, Australia

(Received 18 May 2004; published 15 September 2004)

We report new results of a test of Lorentz invariance based on the comparison of a cryogenic sapphire microwave resonator and a hydrogen-maser. The experimental results are shown together with an extensive analysis of systematic effects. Previously, this experiment has set the most stringent constraint on Kennedy-Thorndike type violations of Lorentz invariance. In this work we present new data and interpret our results in the general Lorentz violating extension of the standard model of particle physics (SME). Within the photon sector of the SME, our experiment is sensitive to seven SME parameters. We marginally improve present limits on four of these, and by a factor seven to ten on the other three.

Lorentz Invariance (LI) is the fundamental postulate of Special Relativity and therefore at the heart of all accepted theories of physics. The central importance of this postulate in modern physics has motivated tremendous work to experimentally test LI with ever increasing precision. Additionally, many unification theories (e.g. string theory or loop gravity) are expected to violate LI at some level [1–3], which further motivates experimental searches for such violations.

Numerous test theories that allow the modeling and interpretation of experiments that test LI have been developed [4–9]. The kinematical frameworks (RMS) of [4,5] postulate a simple parametrization of the Lorentz transformations with experiments setting limits on the deviation of those parameters from their special relativistic values. Owing to their simplicity they have been widely used to model and interpret many experiments that test LI, including our previous publications [10,11]. More recently, a general Lorentz violating extension of the standard model of particle physics (SME) has been developed [8] whose Lagrangian includes all parametrized Lorentz violating terms that can be formed from known fields. Over the last years considerable experimental effort has gone into SME tests [12–14], and the present paper reports our first results in the SME.

In the photon sector of the SME [9], Lorentz violating terms are parametrized by 19 independent components of a tensor $(k_F)_{\kappa\lambda\mu\nu}$ (greek indices run from 0 to 3), which are in general grouped into three traceless and symmetric 3×3 matrices ($\tilde{\kappa}_{e+}$, $\tilde{\kappa}_{o-}$, and $\tilde{\kappa}_{e-}$), one antisymmetric one ($\tilde{\kappa}_{o+}$), and one additional scalar, which all vanish when LI is satisfied. The ten independent components of $\tilde{\kappa}_{e+}$ and $\tilde{\kappa}_{o-}$ are constrained by astronomical measurements to $<2 \times 10^{-32}$ [9]. Seven components of $\tilde{\kappa}_{e-}$ and

$\tilde{\kappa}_{o+}$ have been constrained in an optical cavity experiment [14] at the 10^{-15} and 10^{-11} level, respectively, while the remaining two parameters are unconstrained for the time being. Our experiment is sensitive to the same seven components of $\tilde{\kappa}_{e-}$ and $\tilde{\kappa}_{o+}$ as [14]. It marginally improves present limits on four of these, with significant (factor seven to 10) improvement on the other three.

As already described in [10,11], our experiment consists of a cryogenic sapphire oscillator (CSO) operating in a whispering gallery mode with a resonance frequency of 11.932 GHz which is compared to a commercial (Datum Inc.) active hydrogen-maser (HM). A detailed description can be found in [15–17] with specific details in the context of LI tests in [11].

A standing wave is set up around the circumference of the cylindrical sapphire resonator with the dominant electric and magnetic fields in the radial and vertical directions, corresponding to a propagation (Poynting) vector around the circumference. In the photon sector of the SME the resonant frequency of an electromagnetic (EM) cavity is subject to a Lorentz violating perturbation which can be expressed, to first order, as an integral over the nonperturbed EM fields (eq. (34) of [9]). The change of orientation of the fields due to the rotation and orbital motion of the Earth then provides a time varying modulation of that perturbed frequency, which is searched for in the experiment. As shown in [18] the frequency of the H-maser is not affected to first order (because it operates on $m_F = 0$ states) and [19] shows that the perturbation of the frequency due to the modification of the sapphire crystal structure (and hence the cavity size) is negligible with respect to the direct perturbation of the em fields.

With the above assumptions the perturbed frequency difference ν between the CSO and the H-maser can be expressed in the form (see [11] for a detailed derivation)

$$\frac{\nu - \nu_0}{\nu_0} = \sum_i C_i \cos(\omega_i T_\oplus + \varphi_i) + S_i \sin(\omega_i T_\oplus + \varphi_i) \quad (1)$$

---
*On leave from Bureau International des Poids et Mesures, Pavillon de Breteuil, 92312 Sèvres Cedex, France.

70 051902-1

TABLE I.   Coefficients C_i and S_i in (1) for the six frequencies ω_i of interest and their relation to the components of the SME parameters $\tilde{\kappa}_{e-}$ and $\tilde{\kappa}_{o+}$, with $\omega_\oplus$ and $\Omega_\oplus$ the angular frequencies of the Earth's sidereal rotation and orbital motion. The measured values (in 10^{-16}) are shown together with the statistical (first bracket) and systematic (second bracket) uncertainties.

ω_i	C_i		S_i	
$\omega_\oplus - \Omega_\oplus$	$(-8.6 \times 10^{-6})\tilde{\kappa}_{o+}^{YZ}$	$-6.9(4.2)(4.5)$	$(8.6 \times 10^{-6})\tilde{\kappa}_{o+}^{XZ} - (4.2 \times 10^{-5})\tilde{\kappa}_{o+}^{XY}$	$6.7(4.2)(4.5)$
$\omega_\oplus$	$-0.44\tilde{\kappa}_{e-}^{XZ} + (1.1 \times 10^{-6})\tilde{\kappa}_{o+}^{XZ}$	$14(4.2)(4.2)$	$-0.44\tilde{\kappa}_{e-}^{YZ} + (1.1 \times 10^{-6})\tilde{\kappa}_{o+}^{YZ}$	$2.4(4.2)(4.2)$
$\omega_\oplus + \Omega_\oplus$	$(-8.6 \times 10^{-6})\tilde{\kappa}_{o+}^{YZ}$	$-6.0(4.2)(4.2)$	$(8.6 \times 10^{-6})\tilde{\kappa}_{o+}^{XZ} + (1.8 \times 10^{-6})\tilde{\kappa}_{o+}^{XY}$	$2.7(4.2)(4.2)$
$2\omega_\oplus - \Omega_\oplus$	$(-1.8 \times 10^{-5})\tilde{\kappa}_{o+}^{XZ}$	$3.7(2.4)(3.7)$	$(-1.8 \times 10^{-5})\tilde{\kappa}_{o+}^{YZ}$	$-2.9(2.4)(3.7)$
$2\omega_\oplus$	$-0.10(\tilde{\kappa}_{e-}^{XX} - \tilde{\kappa}_{e-}^{YY})$	$3.1(2.4)(3.7)$	$-0.19\tilde{\kappa}_{e-}^{XY}$	$11(2.4)(3.7)$
$2\omega_\oplus + \Omega_\oplus$	$(7.8 \times 10^{-7})\tilde{\kappa}_{o+}^{XZ}$	$0.0(2.4)(3.7)$	$(7.8 \times 10^{-7})\tilde{\kappa}_{o+}^{YZ}$	$-1.2(2.4)(3.7)$

where ν_0 is the unperturbed frequency difference, the sum is over the six frequencies ω_i of Table I, the coefficients C_i and S_i are functions of the Lorentz violating tensors $\tilde{\kappa}_{e-}$ and $\tilde{\kappa}_{o+}$ (see Table I), $T_\oplus = 0$ on December 17, 2001, 18:05:16 UTC, $\varphi_{\omega_\oplus} = \varphi_{2\omega_\oplus} = 0$ and $\varphi_{(\omega_\oplus \pm \Omega_\oplus)} = \varphi_{(2\omega_\oplus \pm \Omega_\oplus)} = \pm 4.682$ rad.

Our previously published results [10,11] are based on data sets taken between Nov. 2001 and Sept. 2003. All of the data in [10] (except the last data set) were taken before implementation of permanent temperature control of the local environment. As a result the uncertainties in [10] were dominated by the systematic effects from temperature variations. In [11] we have used only data that were permanently temperature controlled yielding an improvement on [10] by about a factor two for the RMS parameters of [4,5]. However, those data were insufficient to decorrelate all seven SME parameters.

In order to do so we have extended the data to 20 data sets in total, spanning Sept. 2002 to Jan. 2004, of differing lengths (5 to 20 days, 222 days in total). The sampling time for all data sets was 100 s. Figure 1 shows the complete data and the power spectral density (PSD) of the longest data set after removal of an offset and a rate
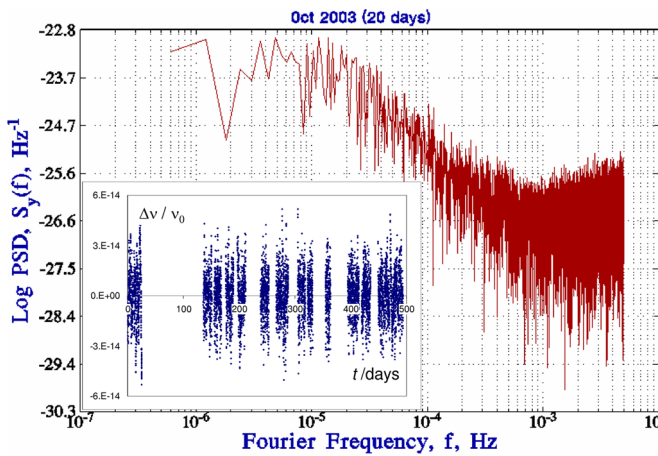

FIG. 1 (color online).   Relative frequency difference between the CSO and the H-maser after removal of a linear fit per data set. Complete data (inset) and PSD of the longest data set.

(natural frequency drift, typically $\approx 1.6 \times 10^{-18}$ s^{-1}) for each data set.

For the statistical analysis we first average the data to 2500 s sampling time and then simultaneously fit the 20 rates and offsets and the 12 parameters C_i and S_i of (1) to the complete data using two statistical methods, weighted least squares (WLS), which allows one to account for nonwhite noise processes (cf. [10]), and individual periods (IP) as used in [14]. The two methods give similar results for the parameters (within the uncertainties) but differ in the estimated uncertainties (the IP uncertainties are a factor ≈ 1.2 larger). Because IP discards a significant amount of data (about 10% in our case) we consider WLS the more realistic method and retain those results as the statistical uncertainties shown in Table I. We note that we now have sufficient data to decorrelate all 12 parameters (C_i, S_i), i.e., the WLS correlation coefficients between any two parameters or between any parameter and the fitted offsets and rates are all less than 0.20.

To investigate the distributions of our results we fit the coefficients C_i and S_i to each one of the 20 data sets individually with the results at the sidereal and semi-sidereal frequencies $\omega_\oplus$ and $2\omega_\oplus$ shown in Fig. 2. If a genuine effect at those frequencies was present we would expect correlated phases of the individual points in Fig. 2, but this does not seem to be supported by the data. A distribution of the phases may result from an effect at a neighboring frequency, in particular, the diurnal and semidiurnal frequencies $\omega_\oplus - \Omega_\oplus$ and $2(\omega_\oplus - \Omega_\oplus)$ at which we would expect systematic effects to play an important role. Figure 3 shows the amplitudes $A_\omega = \sqrt{C_\omega^2 + S_\omega^2}$ resulting from least squares fits for a range of frequencies ω around the frequencies of interest. We note that the fitted amplitudes at $\omega_\oplus - \Omega_\oplus$ and $2(\omega_\oplus - \Omega_\oplus)$ are substantially smaller than those at $\omega_\oplus$ and $2\omega_\oplus$ and therefore unlikely to contribute to the distribution of the points in Fig. 2.

Systematic effects at the frequencies ω_i could mask a putative Lorentz violating signal in our experiment and need to be investigated in order to be able to confirm such a signal or to exclude it within realistic limits. We have extensively studied all systematic effects arising from environmental factors that might affect our experiment.
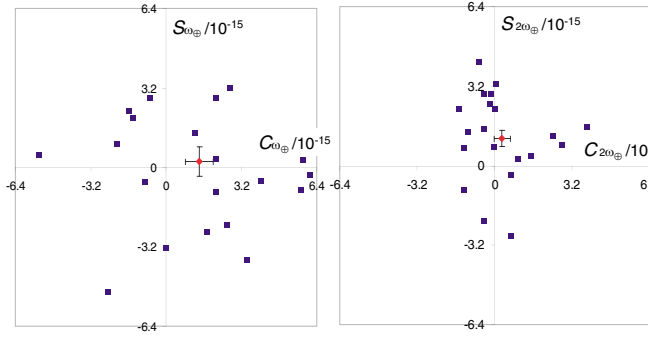
FIG. 2 (color online). Fitted sine and cosine amplitudes at $\omega_\oplus$ and $2\omega_\oplus$ for each data set (squares) and the complete data (diamonds, with statistical errors). For clarity the error bars of the individual data sets have been omitted.

The resulting estimated contributions at the two central frequencies $\omega_\oplus$, $2\omega_\oplus$ and at the diurnal frequency $\omega_\oplus - \Omega_\oplus$ are summarized in Table II. The contributions at $\omega_\oplus + \Omega_\oplus$ and $2\omega_\oplus \pm \Omega_\oplus$ are not shown as they are identical to those at $\omega_\oplus$ and $2\omega_\oplus$ respectively.

We have compared the HM used as our frequency reference to our highly stable and accurate Cs-fountain clocks (FO2 and FOM). For example, the amplitudes at $\omega_\oplus$ and $2\omega_\oplus$ of the HM-FOM relative frequency difference over June-July 2003 were $A_{\omega_\oplus} = (4.8 \pm 4.7) \times 10^{-16}$ and $A_{2\omega_\oplus} = (4.3 \pm 4.7) \times 10^{-16}$. This indicates that any environmental effects on the HM at those frequencies should be below five parts in 10^{16} in amplitude. This is in good agreement with studies on similar HMs carried out in [20] that limited environmental effects to $<$ three to four parts in 10^{16}.

To estimate the tilt sensitivity we have intentionally tilted the oscillator by ≈ 5 mrad off its average position which led to relative frequency variations of $\approx 3 \times 10^{-13}$ from which we deduce a tilt sensitivity of $\approx 6 \times 10^{-17}$ μrad^{-1}. This is in good agreement with similar measurements in [17] that obtained sensitivities of $\approx 4 \times 10^{-17}$ μrad^{-1}. Measured tilt variations in the lab at diurnal and semidiurnal periods show amplitudes of 4.6 μrad
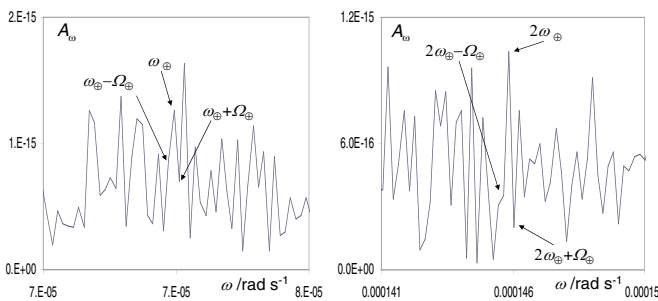

FIG. 3 (color online). Fitted Amplitudes A_ω for a range of frequencies around the six frequencies ω_i of interest (indicated by arrows).

TABLE II. Contributions from systematic effects to the amplitudes A_i (parts in 10^{16}) at three frequencies ω_i.

Effect	$\omega_\oplus - \Omega_\oplus$	$\omega_\oplus$	$2\omega_\oplus$
H-maser	<5	<5	<5
Tilt	3	3	1
Gravity	0.3	0.3	0.3
B-field	<0.1	<0.1	<0.1
Temperature	<1	<1	<1
Atm. Pressure	2.3	0.3	0.4
Total	**6.4**	**5.9**	**5.2**

and 1.6 μrad, respectively, which leads to frequency variations that do not exceed 3×10^{-16} and 1×10^{-16}, respectively.

From the measurements of tilt sensitivity one can deduce the sensitivity to gravity variations (cf. [17]), which in our case lead to a sensitivity of $\approx 3 \times 10^{-10}$ g^{-1}. Tidal gravity variations can reach $\approx 10^{-7}$ g from which we obtain a maximum effect of 3×10^{-17}, one order of magnitude below the effect from tilt variations.

Variations of the ambient magnetic field in our lab are dominated by the passage of the Paris Metro, showing a strong periodicity ("quiet" periods from 1:00 a.m. to 5:00 a.m.). The corresponding diurnal and semidiurnal amplitudes are 1.7×10^{-4} G and 3.4×10^{-4} G, respectively, for the vertical field component and about 10 times less for the horizontal one. To determine the magnetic sensitivity of the CSO we have applied a sinusoidal vertical field of 0.1 G amplitude with a 200 s period. Comparing the CSO frequency to the FO2 Cs-fountain we see a clear sinusoidal signal (S/N >2) at the same period with an amplitude of 7.2×10^{-16}, which leads to a sensitivity of $\approx 7 \times 10^{-15}$ G^{-1}. Assuming a linear dependence (there is no magnetic shielding that could lead to nonlinear effects) we obtain effects of only a few parts in 10^{-18}.

In late 2002 we implemented an active temperature stabilization inside an isolated volume (≈ 15 m^3) that includes the CSO and all the associated electronics. The temperature is measured continuously in two fixed locations (behind the electronics rack and on top of the Dewar). For the best data sets the measured temperature variations do not exceed 0.02/0.01 K in amplitude for the diurnal and semidiurnal components. A least squares fit to all our temperature data (taken simultaneously with our frequency measurements) yields amplitudes of $A_{\omega_\oplus} = 0.020$ K and $A_{2\omega_\oplus} = 0.018$ K with similar values at the other frequencies ω_i of interest, including the diurnal one ($A_{\omega_\oplus - \Omega_\oplus} = 0.022$ K). Inducing a strong sinusoidal temperature variation (≈ 0.5 K amplitude at 12 h period) leads to no clearly visible effect on the CSO frequency. Taking the noise level around the 12 h period as the maximum effect we obtain a sensitivity of $<4 \times 10^{-15}$

per K. Using this estimate we obtain effects of $<1 \times 10^{-16}$ at all frequencies ω_i.

Finally we have investigated the sensitivity of the CSO to atmospheric pressure variations. To do so we control the pressure inside the Dewar using a variable valve mounted on the He gas exhaust. During normal operation the valve is open and the CSO operates at ambient atmospheric pressure. For the sensitivity determination we have induced a sinusoidal pressure variation (≈ 14 mbar amplitude at 12 h period), which resulted in a clearly visible effect on the CSO frequency corresponding to a sensitivity of $\approx 6.5 \times 10^{-16}$ mbar^{-1}. We have checked that the sensitivity is not significantly affected when changing the amplitude of the induced pressure variation by a factor 3. A least squares fit to atmospheric pressure data (taken simultaneously with our frequency measurements) yields amplitudes of $A_{\omega_\oplus} = 0.045$ mbar and $A_{2\omega_\oplus} = 0.054$ mbar with similar values at the other frequencies ω_i of interest, except the diurnal one for which $A_{\omega_\oplus - \Omega_\oplus} = 0.36$ mbar. The resulting effects on the CSO frequency are given in Table II.

Our final results for the seven components of $\tilde{\kappa}_{e-}$ and $\tilde{\kappa}_{o+}$ are obtained from a least squares fit to the 12 measured coefficients of Table I. They are summarized and compared to the results of [14] in Table III.

We note that our results for $\tilde{\kappa}_{e-}^{XY}$ and $\tilde{\kappa}_{e-}^{XZ}$ are significant at about 2σ, while those of [14] are significant at about the same level for $(\tilde{\kappa}_{e-}^{XX} - \tilde{\kappa}_{e-}^{YY})$. The two experiments give compatible results for $\tilde{\kappa}_{e-}^{XZ}$ (within the 1σ uncertainties) but not for the other two parameters, so the measured values of those are unlikely to come from a common

TABLE III. Results for the components of the SME Lorentz violation parameters $\tilde{\kappa}_{e-}$ (in 10^{-15}) and $\tilde{\kappa}_{o+}$ (in 10^{-11}).

	$\tilde{\kappa}_{e-}^{XY}$	$\tilde{\kappa}_{e-}^{XZ}$	$\tilde{\kappa}_{e-}^{YZ}$	$(\tilde{\kappa}_{e-}^{XX} - \tilde{\kappa}_{e-}^{YY})$
from [14]	1.7(2.6)	-6.3(12.4)	3.6(9.0)	8.9(4.9)
this work	-5.7(2.3)	-3.2(1.3)	-0.5(1.3)	-3.2(4.6)

	$\tilde{\kappa}_{o+}^{XY}$	$\tilde{\kappa}_{o+}^{XZ}$	$\tilde{\kappa}_{o+}^{YZ}$
from [14]	14(14)	-1.2(2.6)	0.1(2.7)
this work	-1.8(1.5)	-1.4(2.3)	2.7(2.2)

source. Another indication for a nongenuine effect comes from Figs. 2 and 3 as we would expect any genuine effect to show an approximately coherent phase for the individual data sets in Fig. 2. and to display more prominent peaks in Fig. 3.

In conclusion, we have not seen any Lorentz violating effects in the general framework of the SME, and set limits on seven parameters of the SME photon sector (cf. Table III) which are up to an order of magnitude more stringent than those obtained from previous experiments [14]. Two of the parameters are significant (at $\approx 2\sigma$). We believe that this is most likely a statistical coincidence or a neglected systematic effect. To verify this, our experiment is continuing and new, more precise experiments are under way [21].

[1] V. A. Kostelecký and S. Samuel, Phys. Rev. D **39**, 683 (1989).
[2] T. Damour, gr-qc/9711060.
[3] R. Gambini and J. Pullin, Phys. Rev. D **59**, 124021 (1999).
[4] H. P. Robertson, Rev. Mod. Phys. **21**, 378 (1949).
[5] R. Mansouri and R. U. Sexl, Gen. Relativ. Gravit. **8**, 497 (1977).
[6] A. P. Lightman and D. L. Lee, Phys. Rev. D **8**, 364 (1973).
[7] W.-T. Ni, Phys. Rev. Lett. **38**, 301 (1977).
[8] D. Colladay and V. A. Kostelecký, Phys. Rev. D **55**, 6760 (1997); and , **58**, 116002 (1998); V. A. Kostelecký, Phys. Rev. D **69**, 105009 (2004).
[9] V. A. Kostelecký and M. Mewes, Phys. Rev. D **66**, 056005 (2002).
[10] P. Wolf et al., Phys. Rev. Lett. **90**, 060402 (2003).
[11] P. Wolf et al., Gen. Relativ. Gravit. **36**, 2351 (2004).
[12] CPT and Lorentz Symmetry II, edited by V. A. Kostelecký (World Scientific, Singapore, 2002).
[13] J. A. Lipa et al., Phys. Rev. Lett. **90**, 060403 (2003).
[14] H. Müller et al.,,, Phys. Rev. Lett. **91**, 020401 (2003).
[15] S. Chang, A. G. Mann, and A. N. Luiten, Electron. Lett. **36**, 480 (2000).
[16] A. G. Mann, S. Chang, and A. N. Luiten, IEEE Trans. Instrum. Meas. **50**, 519 (2001).
[17] S. Chang, Ph.D. thesis, Univ. of West. Aus., 2000.
[18] V. A. Kostelecký and C. D. Lane, Phys. Rev. D **60**, 116010 (1999).
[19] H. Müller et al., Phys. Rev. D **67**, 056006 (2003).
[20] T. E. Parker, IEEE Trans. Ultrason. Ferroelectr. Freq. Control **46**, 745 (1999).
[21] M. E. Tobar et al., Phys. Lett. A **300**, 33 (2002).